CHAPITRE 4 : Transport d'acides nucléiques dans les cellules endothéliales cérébrales via l'utilisation de complexes micellaires polyioniques ciblant le récepteur de la transferrine

Résumé

Les cellules endothéliales du cerveau (CECCs) sont une composante essentielle de la barrière hémato-encéphalique (BHE) d'un point de vue structural et fonctionnel. Le transport de composés biopharmaceutiques dans les CECCs pourrait avoir un potentiel thérapeutique pour les pathologies du cerveau. Les micelles polyioniques sont reconnues pour leur capacité à relâcher leur contenu en acides nucléiques suite à l'acidification du pH ainsi que pour leurs propriétés de ciblage nucléaire. Dans cette étude, étudié l'accumulation cellulaire de micelles polyioniques contentant un petit ARN double brin fluorescent (siGLO) *in vitro* et *in vivo* conjuguées avec un fragment Fab' (Ri7) ciblant le récepteur de la transferrine (RTf). Les expériences menées sur des cellules N2A ont montré une internalisation spécifique au RTf à 37^{o}C. La colocalisation du signal provenant du siGLO avec le RTf est demeurée relativement constante sur une période de 24 h. D'autres expérimentations ont aussi montré une colocalisation partielle avec le marqueur des endosomes précoces (EEA-1) et des lysosomes (LAMP-1), et ce malgré une augmentation de la colocalisation entre les micelles et le marqueur LAMP-1 après 4 h d'incubation. L'administration systémique des micelles chez la souris a montré une accumulation uniforme dans les CECCs demeurant soutenues jusqu'à 8 h après l'injection. L'apparence du signal fluorescent du siGLO Red sous forme de points suggère que les micelles ciblant le RTf sont incorporées dans les compartiments intracellulaires comme les endosomes. L'administration systémique de pARNi ciblant la protéine GAPDH complexés dans les micelles polyioniques ciblant le RTf n'a pas mené à la baisse des niveaux de protéines de GAPDH. Cependant, nos résultats suggèrent tout de même que les micelles polyioniques ciblant le RTf sont capables de conduire à une accumulation d'acides nucléiques dans les CECCs.

Brain endothelial cells delivery of nucleic acids using transferrin receptor-targeted polyion complex micelles

Sarah Paris-Robidas[1,2], Philippe Bourassa[1,2], Aurélie Louit[1,2], Arnaud Felber[3], Vincent Émond[1,2], Denis Soulet[2,3], Jean-Christophe Leroux[4], Frédéric Calon[1,2*]

[1]Faculty of Pharmacy, Laval University, Quebec (Qc), Canada

[2]CHU Research Center, Neurosciences Axis, Quebec (QC), Canada

[3]Faculty of Medecine, Laval University, Quebec (Qc), Canada

[4]Department of Chemistry and Applied Biosciences, Institute of Pharmaceutical Sciences, ETH Zurich, Zurich, Switzerland

Running title: BCECs accumulation of siRNA

Abstract

Brain capillary endothelial cells (BCECs) are a major structural and functional component of the blood-brain barrier (BBB). Delivery of biopharmaceuticals into BCECs has therapeutic potential in prevalent brain disorders. Polyion complex micelles (PICMs) are recognized for their ability to release their nucleic acid core under acidic conditions and for their transfection efficacy. Here, we encapsulated a fluorescent double-stranded RNA (siGLO Red) in pH-sensitive PICMs conjugated with Fab' antibody fragments (clone Ri7) targeting the murine transferrin receptor (TfR) and investigated the cellular uptake of PICMs *in vitro* and *in vivo*. Experiments conducted *in vitro* showed TfR-specific internalization of Fab'Ri7-PICM-siGLO in murine neuro-2a neuroblastoma cells at 37°C. The siGLO Red signal was localized extensively in sorting/recycling (TfR-positive) endosomes over 24 h, reaching maximal colocalization at 4 h. On the other hand, early (EEA1-positive) endosomal and lysosomal (LAMP-1-positive) colocalization of the siGLO Red signal remained low, despite an increase that was gradual in early endosomes and more abrupt in lysosomes after 4 h of incubation. Systemic intravenous administration in mice showed a rapid accumulation of siGLO Red within BCECs that remained high 8 h after a single injection. The punctate fluorescent signal suggests that Fab'Ri7-PICM were incorporated into intracellular compartments such as endosomes. However, systemic administration of Fab'RI7-PICM complexed with siRNA targeting GAPDH did not lead to reduction of GAPDH protein levels in isolated brain microvessels. These findings demonstrate that TfR-targeted pH-sensitive PICMs can ferry nucleic acids into BCECs.

Graphical abstract

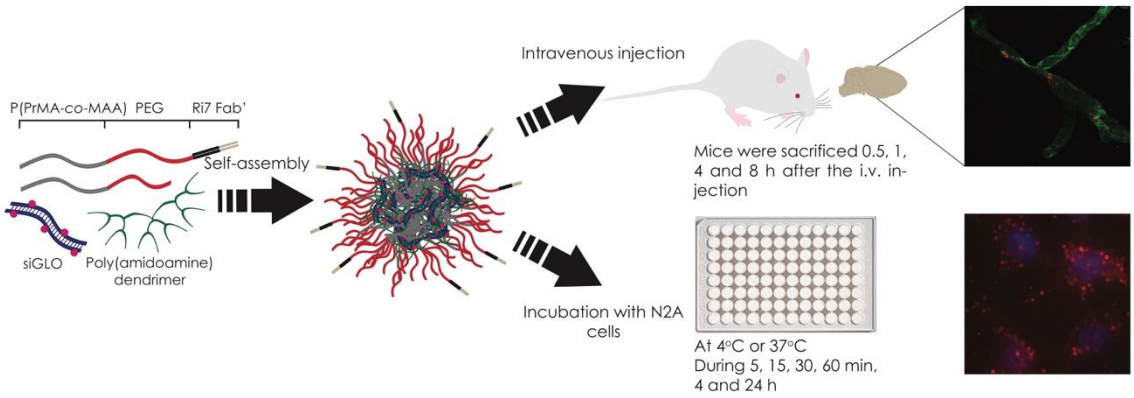

Keywords: Blood-brain barrier, transferrin receptor, polyionic complex micelle, brain capillary endothelial cells, drug delivery

Introduction

Brain capillary endothelial cells (BCECs) are a major structural and functional component of the blood-brain barrier (BBB) (Blanchette et al. 2015, Zhao et al. 2015). On the one hand, BCECs form a static and metabolic barrier preventing biopharmaceutical compounds to reach the brain in therapeutic concentrations (Pardridge 2007c, Abbott 2013, Watts et al. 2013, Blanchette et al. 2015, Zhao et al. 2015). It has been estimated that 98% of potential neurotherapeutics cannot cross the BBB (Pardridge 2007a, Pardridge 2012). On the other hand, BCECs are potential gateways (Jiang et al. 2003, Paris-Robidas et al. 2011, Paris-Robidas et al. 2016) that closely embrace the extensive vascular network encompassing the whole brain parenchyma (Oldendorf 1977, Pardridge 2007b, Pardridge 2012). Indeed, BCECs are a dynamic component of the neurovascular unit that express a wide array of specific receptors involved in receptor-mediated transcytosis/endocytosis (Descamps et al. 1996, Fillebeen et al. 1999, Demeule et al. 2002, Cornford et al. 2005). Moreover, recent publications have highlighted the intrinsic role played by BCECs in prevalent brain disorders such as neurodegenerative diseases or stroke (Zlokovic 2002, Bell et al. 2007, Bell et al. 2009, Winkler et al. 2015). Therefore, a drug that directly targets BCECs could potentially treat brain diseases.

Gene therapy has become an attractive strategy for the treatment of CNS disorders, but cerebral delivery of nucleic acids following systemic administration still represents a challenge (Gomes et al. 2015, Lorenzer et al. 2015). Recent advances in biopharmaceutical nanotechnology have led to the design of polyion complex micelles (PICMs), which are nanoparticles typically generated by the interactions between nucleic acids and a diblock copolymer (Kataoka et al. 1996, Yessine et al. 2007). We previously generated a novel PICM formulation based on the reversible interaction between a diblock copolymer poly(ethylene glycol)-*b*-poly(propyl methacrylate-*co*-methacrylate acid) (PEG-*b*-p(PrMA-*co*-MAA) and conventional poly(amido amine) (PAMAM) dendrimers, forming a 50-60 nm pH-sensitive nanocarrier (Felber et al. 2011). Upon cellular uptake via receptor-mediated endocytosis, the acidic pH in endosomal compartments protonates carboxylate groups of the MAA, thereby destabilizing the core of the PICM. The protonated MAA copolymer and the remaining unprotected PAMAM-nucleic acid core then promote endosomal escape by interacting with the endosomal membrane and/or via the proton sponge effect (Yessine et al. 2003, Dufes et al. 2005, Hong et al. 2006), which can ultimately translate into gene silencing, as evidenced previously in with

small interfering (si) RNA in PC-3 cells (Elsabahy et al. 2009, Felber et al. 2011).

Owing to its localization on the lumen of BCECs, the transferrin receptor (TfR) is one of the most studied potential transport systems for brain drug delivery (Friden et al. 1991, Bickel et al. 1994, Zhang et al. 2003b, Ulbrich et al. 2009). In the past 20 years, preclinical successes have been reported using vectors targeting the TfR in rodents (Shin et al. 1995, Shi et al. 2000, Shi et al. 2001b, Zhang et al. 2006, Yu et al. 2011, Yu et al. 2014). Ri7.217 (Ri7) is a rat monoclonal antibody (mAb) raised against the murine TfR, originally developed to study the implication of TfR on cellular proliferation (Lesley et al. 1984b). However, Ri7 has been shown to accumulate in the brain after systemic injection (Shin et al. 1995, Shi et al. 2000, Paris-Robidas et al. 2011, Johnsen et al. 2016). Fluorescence and electron microscopy studies showed that systemic administration of TfR-specific Ri7 mAbs leads to their massive internalization in BCECs, thus highlighting their potential as a BCEC-targeting vector (Paris-Robidas et al. 2011, St-Amour et al. 2013, Paris-Robidas et al. 2016). (Alata et al. 2014)

Material and methods

Diblock copolymer synthesis

Non-targeted $mPEG_{115}$-*b*-P(PrMA-*co*-MAA) was synthesized by atom transfer radical polymerization (ATRP) as previously described using a methoxy-PEG_{115} (M_n = 5000 g mol^{-1})(Sant et al. 2004). Fab'-PEG_{169}-*b*-P($PrMA_{31}$-*co*-MAA_{62}) copolymer was synthesized starting from H_2N- PEG_{169}-OH 1 (M_n = 7500). Briefly, H_2N-PEG_{169}-OH 1 was protected using di-tert-butyl dicarbonate (2.5 eq., dissolved in acetonitrile) and NaOH (3 eq., 0.1 M) for 2 h. The resulting product 2 was acylated with 2-bromoisobutyryl bromide using a previously reported procedure to afford the macroinitiator(Ranger et al. 2001). The polymerization reactions were carried out by ATRP, using PrMA and tBMA, under conditions reported previously(Sant et al. 2004). H_2N-PEG_{169}-*b*-P($PrMA_{31}$-*co*-MAA_{62}) 4 was obtained by deprotection of the tert-butyl carbamate and tert-butyl ester in trifluoroacetic acid and dimethyl sulfoxide (DMSO) 5/95 (v/v), followed by purification by dialysis against water for 2 days (MWCO of 3.5 kDa). The purified polymer was recovered by lyophilization of the aqueous solution. The yield of polymerization/ deprotection steps was approximately 50%. The maleimide bifunctional linker, N-[γ-maleimidobutyryloxy]-sulfosuccinimide ester (sulfo-GMBS, 10 eq), was reacted with polymer 4 overnight in phosphate buffered saline 10 mM (PBS 1X) pH 7.2. Excess linker was removed using a membrane with a 3-kDa molecular weight cutoff (Millipore, Billerica, MA), and product 5 was recovered by lyophilization. The final active maleimide content of the polymer was approximately 60% as determined by ^{1}H NMR spectroscopy. Selected ^{1}H-NMR resonance (D_2O, 400 MHz) δ: 6.85 (s, maleimide), 3.96 (br m, OCH_2 in PrMA), 3.75 (m, OCH_2CH_2 in PEG chain), 2.20–1.60 (br, CH_2 in the PrMA and polymer backbone), 1.15–0.80 (br, CH_3 groups in PrMA and MAA). Anti-transferrin receptor antibody (Ri7.217) (Bio X Cell, West Lebanon, NH) was digested to F(ab')$_2$ following the mouse IgG1 Fab and F(ab')$_2$ preparation kit procedure (Pierce, Rockford, IL) and purified by FPLC. Maleimide-PEG_{169}-*b*-P($PrMA_{31}$-*co*-MAA_{62}) 5 was coupled to the freshly reduced Fab'-SH (1.5 eq.) overnight in degassed PBS at pH 7.2. Excess Fab' was removed through an anion exchange column (HiTrap Q FF, GE Healthcare, Glattbrugg, Switzerland), and the product concentration was determined by the bicinchoninic acid (BCA) protein assay (Pierce). Unreacted maleimide groups were quenched with cysteine (5 eq). The final Fab'-PEG_{169}-*b*-P($PrMA_{31}$-*co*-MAA_{62}) Finally, the purity

was assessed by sodium dodecyl sulfate poly(acrylamide) gel electrophoresis (SDS-PAGE).

PICM preparation

Briefly, negatively charged micelle components (PEG_{115}-*b*-P(PrMA-*co*-MAA), Fab'-PEG_{169}-*b*-P($PrMA_{31}$-*co*-MAA_{62}) and dsRNA (either siGLO Red from GE Dharmacon or Silencer Select GAPDH positive control siRNA from Ambion/ThermoFisher) were combined in Tris buffer (10 mM, pH 7.4) and mixed with PAMAM dendrimer to obtain a N/(P+COOH) molar ratios of 2.0. N corresponds to the number of primary amine groups of the PAMAM while P and COOH account for the phosphate and carboxylate groups of the nucleic acid and MAA copolymer, respectively. The samples were stirred for 20 min at room temperature (RT°) to allow micelle formation.

4°C vs 37°C experiments

Murine neuroblastoma (neuro-2a, N2A, #CCL-131, ATCC, Manassas, VA) cells were seeded in 96-well plates containing Dulbecco's modified Eagle medium (DMEM) supplemented with 10% fetal bovine serum (FBS) at 4 x 10^5 cells per well. Two days later, medium was removed and cells were incubated with Fab'Ri7-PICM or UT-PICM (negative control, untargeted PICMs) containing 500 nM of siGLO-Red, a chemically synthesized double-stranded (ds) RNA analog (Dharmacon, Ottawa, ON, Canada) during 30 min at 4°C or 37°C. Afterwards, cells were washed once with cold DMEM-FBS 10%, twice with cold 1X Dulbecco's (D)-PBS containing Mg^{2+} and Ca^{2+}, fixed with 4% paraformaldehyde (PFA) and incubated with the DAPI nuclear stain (Sigma-Aldrich, Oakville, ON, Canada). Images were acquired with an EVOS™ FL auto imaging system (ThermoFisher Scientific, Waltham, MA).

In vitro competition studies

N2A cells were seeded in 96-well plates containing DMEM supplemented with 10% FBS at 5 x 10^5 cells per well. The next day, medium was removed and cells were preincubated with Ri7 or control IgG (2a3, BioXCell) (0, 50 or 200 nM) for 30 min. Then, Fab'Ri7-PICM were added to a final siGLO-Red (Dharmacon) concentration of 250 nM and incubation was resumed for 15 min. Incubation was terminated by removal of PICMs and sequential washes with ice-cold DMEM-FBS 10% and D-PBS 1X. Afterwards, cells were fixed with 4% PFA, cell nuclei were counterstained with DAPI (Sigma-

Aldrich) and IBIDI mounting media was added. Each condition was performed in triplicates. Images were acquired with an EVOS™ FL auto imaging system (ThermoFisher Scientific). Quantification of the siGLO-Red fluorescent signal was performed using the triangle thresholding method in ImageJ (National Institutes of Health, Bethesda, MD). For each condition, 9-12 micrographs taken at a 20x magnification were quantified.

In vitro Fab'Ri7-PICM kinetics of internalization and colocalization analyses

N2A cells were seeded in 96-well plates containing DMEM supplemented with 10% FBS at 4 x 10^5 cells per well. Two days later, medium was removed and cells were incubated with DMEM-10% FBS containing Fab'Ri7-PICM or UT-PICM containing siGLO-Red (500 nM) for 5, 15, 30, 60 min, 4 and 24 h. Afterwards, cells were washed with cold DMEM-10% FBS, 1X D-PBS, fixed with 4% PFA and cell nuclei were stained with DAPI (Sigma-Aldrich). For colocalization analyses, a similar protocol was used with µ-Slide VI$^{0.4}$ chamber slides (IBIDI, Munich, Germany), where N2A cells (1.2 x 10^4 cells per well) were incubated with Fab'Ri7-PICM containing siGLO-Red for 5 min to 24 h. Afterwards, cells were washed with ice-cold DMEM-FBS 10%, 1X D-PBS and fixed with 4% PFA for 15 min. Following fixation, cells were permeabilized with D-PBS containing 0.5% Triton X-100 for 10 min and blocked with a 3% bovine serum albumin (BSA), 3% normal horse serum (NHS) and 0.05% Triton X-100 during 45 min. Cells were then incubated overnight at 4°C with primary antibodies in a D-PBS solution containing 1% BSA, 1% NHS and 0.05% Triton X-100 : rabbit anti-early endosome antigen 1 (EEA1, 1:200, NEB Cell Signaling, ON, Canada), rabbit anti-TfR ab84036 (1:200, Abcam, ON, Canada) and rabbit anti-LAMP-1 (1:2000, Sigma-Aldrich, ON, Canada). Following incubation with primary antibodies, cells were exposed to Alexa-Fluor™-conjugated donkey anti-rabbit secondary antibodies (ThermoFisher Scientific), cell nuclei were counterstained with DAPI (Sigma-Aldrich) and IBIDI mounting media was added. Colocalization analysis was performed with Bitplane Imaris 7.5.1 colocalization module using the Costes' estimation for automatic threshold, which compares the Pearson's coefficient for non-randomized vs. randomized images and calculates the significance (Costes et al. 2004).

Animals

Adult Tie2GFP mice (Jackson Laboratory, Bar Harbor, ME) weighing 20-30 g at 4-6 months of age

were used. They had ad libitum access to food and water. These mice express green fluorescent protein in endothelial cells. All procedures were performed in accordance with the Canadian Council on Animal Care standards and were approved by the Animal Ethics Committee of the *Centre Hospitalier de l'Université Laval* (CHUL).

Tissue preparation for post-mortem analysis

For microscopy experiments, mice were administered in the tail vein with Fab'Ri7-PICM or UT-PICM containing 40 µg (1.33 mg/kg) of siGLO-Red and sacrificed 0.5, 1, 4, 8 h post injection by terminal transcardiac perfusion under deep anesthesia with ketamine/xylazine. Animals were perfused with 25 ml of cold 1X PBS followed by 50 ml of cold 4% PFA, pH 7.4. Brains were rapidly dissected, post-fixed with 4% PFA for 4 h and cut in coronal sections of 25 µm with a microtome (Leica Microsystems, Richmond Hill, ON, Canada). For quantification of GAPDH and TfR levels, animals were injected systemically every 12 h during 36 h with Fab'Ri7-PICM containing 50 µg of anti-GAPDH or Silencer Select negative control #1 siRNA and sacrificed by transcardiac perfusion with 1X PBS containing protease inhibitors (SigmaFast protease inhibitor tablets, Sigma-Aldrich) 24 h following the last injection. Brain and liver were collected and weighed.

Brain microvessels isolation

Brain microvessels of mice were isolated by density-gradient centrifugation using the capillary depletion technique as previously described (Alata et al. 2015; Do et al. 2014). Briefly, brains were collected and transferred into ice-cold 1X PBS. Cerebellum, meninges and brain stem were removed. The brain was gently homogenized in ice-cold DMEM containing 10% FBS using a Potter homogenizer. Homogenates were centrifuged at 500 g for 10 minutes at 4°C, the supernatant was excluded and the pellets were homogenized in 5 mL of ice-cold DMEM containing 25% BSA and centrifuged at 1,500 g for 20 minutes at 4°C. The resulting pellets were resuspended in 1 mL of cold DMEM, 10% FBS and the homogenate were filtered through a 60-µm filter. Filtrates were centrifuged at 12,000 g for 45 minutes at 4°C. Pellets containing the microvessels were washed in ice-cold 1X PBS and centrifuged again at 12,000 g for 20 minutes at 4°C. Supernatants were discarded and the pellets were stored at - 80°C until processing for Western blotting analysis.

Protein extraction

Proteins were extracted from tissues as previously described (Alata et al. 2015). Briefly, the pellet containing cerebral microvessels was weighed and total proteins were extracted by homogenization in four volumes of lysis buffer (150 mmol/L NaCl, 10 mmol/L NaH_2PO_4, 1% Triton X-100, 0.5% SDS, and 0.5% deoxycholate, pH 7.4) containing Complete protease inhibitors (Roche, Indianapolis, IN) and 10 mg/mL pepstatin A. The obtained suspension was sonicated briefly (3×10 seconds) and centrifuged at 100,000g for 20 minutes at 4°C. Protein concentrations were determined with the BCA assay and supernatants were stored at -80°C until Western blotting analysis.

Western Blotting

Equal amounts of proteins per sample were added to Laemmli's loading buffer, heated to 95°C for 5 minutes before loading (15 µg protein per lane), and subjected to sodium dodecyl sulfate-polyacrylamide (SDS) gel electrophoresis (St-Amour et al. 2014). Proteins were electroblotted onto PVDF membranes (Immobilon, Millipore, MA) before blocking in 5% non-fat dry milk, 0.5% BSA, and 0.1% Tween-20 in 1X PBS for 1 h at RT°. The membranes were washed three times for 10 minutes in 1X PBS containing 0.1% Tween-20. Then, membranes were incubated overnight at 4°C with mouse anti-GAPDH (1:5000, ABM, BC, Canada) or rabbit anti-TfR primary antibody (1:1000, Abcam, ON, Canada) diluted in 1X PBS containing 0.1% Tween-20, 5% non-fat dry milk, and 0.5% BSA. The next day, membranes were washed three times for 10 minutes in 1X PBS containing 0.1% Tween-20 and then incubated for 1 h at RT° with goat anti-mouse or anti-rabbit horseradish peroxidase-labeled (1:60 00, Jackson, West Grove, PA) secondary antibodies diluted in 1X PBS containing 0.1% Tween-20 and 1% BSA. Membranes were again washed three times for 10 minutes in 1X PBS containing 0.1% Tween-20 and probed with chemiluminescence reagents (Luminata, ThermoFisher). Immunoblots were analyzed with a KODAK Imaging Station 4000MM Digital Imaging System (Molecular Imaging Software version 4.0.5f7, Carestream Health, Rochester, NY).

Immunofluorescence

Washing steps were performed using 1X PBS, pH 7.4, between every step of the immunofluorescence protocol. Coronal brain sections were blocked for 1 h with a 1X PBS solution containing 5% NHS and 0.2% Triton X-100. Afterwards, sections were incubated overnight at 4^{o}C with primary antibodies in the blocking solution: rabbit anti-GFP (1:1000, A-11122, ThermoFisher Scientific), mouse anti-neuronal nuclei (1:1000, NeuN, Chemicon/Milipore, Temecula, CA) and mouse anti-aquaporine-4 (1:100, Abcam). Following incubation with primary antibodies, slices were exposed to Alexa Fluor conjugated donkey anti-mouse and anti-rabbit secondary antibodies (1:1000, ThermoFisher Scientific). After transfer of onto SuperFrost Plus slides (ThermoFisher Scientific), brain sections were treated with 3 mM $CuSO_4$ in ammonium acetate buffer to minimize brain autofluorescence due to cellular accumulation of lipofuscines (Schnell et al. 1999). Finally, slides were coverslipped with ProLong® Diamond antifade media (ThermoFisher Scientific).

Data and statistical analysis

Competition *in vitro* experiments were performed in triplicate. ANOVA followed by a Tukey post-hoc test was used to detect significant differences between groups when appropriate. Statistical significance was set at * $p< 0.05$, *** $p< 0.001$ and **** $p < 0.0001$. All statistical analyses were performed using Prism 5 for Macintosh (GraphPad Software Inc., San Diego, CA).

Results

Fab'Ri7-PICMs accumulate in brain endothelial cells in vivo

Our previous publications demonstrated the capacity of clone Ri7 to both target and internalize in BCECs (Paris-Robidas et al. 2011, St-Amour et al. 2013, Paris-Robidas et al. 2016). To investigate brain cellular distribution of these novel nanoparticles, we performed confocal microscopy analyses after systemic injection of Fab'Ri7- and UT-PICM containing siGLO-Red in Tie2GFP mice, 0.5, 1, 4 and 8 h post injection. Images shown in Figure 27 indicate that the siGLO encapsulated in Fab'Ri7-PICM was delivered into the cerebral vasculature. The siGLO Red fluorescent signal started to accumulate 30 min post-injection and remained up to 8 h post injection, and no visible fluorescent signal was observed in animals injected with UT-PICM. Despite the clear vascular accumulation of Fab'RI7-PICM, scarce accumulation of the siGLO Red signal was visible in the brain parenchyma (Figure 28, shown by arrows). To determine whether Fab'Ri7-PICM had reached others cell type expressing the TfR present in the brain, we performed colocalization analyses by immunofluorescence with astrocytical endfeet and neuronal markers, AQP-4 and NeuN, respectively (Figure 28). Images acquired by confocal microscopy showed scarce evidence of colocalization with astrocytes (B) and neurons (D) suggesting that only a minor proportion of Ri7-PICM was exocytosed on the abluminal side of BCECs.

Fab'Ri7-PICM-siRNA and GAPDH knockdown in vivo

To investigate if the cerebrovascular accumulation of siGLO could be translated by *in vivo* gene silencing efficacy, mice were injected with 50 µg of anti-GAPDH (siGAPDH) or negative control siRNA every 12 h during 36 h. Quantification by Western blot showed no significant knockdown in either brain capillaries or liver in mice injected with Fab'Ri7-PICM-siGAPDH (Figure 29A-B). Previous publication suggested that the systemic administration of high-affinity mAb targeting the TfR could lead to the degradation of TfR and thus impaired therapeutic of such mAbs (Lesley et al. 1984b, Bien-Ly et al. 2014). To verify whether repeated administration of Fab'Ri7-PICM led to a compensatory decrease in TfR that could limit nanoparticle entry, Tie2GFP mice were injected twice a day for two days with Fab'Ri7-PICM containing negative control siRNA. Quantification by Western

blot on capillary depletion fractions and liver showed no significant difference on TfR levels between mice injected with Fab'Ri7-PICM and control uninjected mice (Figure 29C-D). Our data suggest that the uptake of Ri7-targeted nanoparticles through the TfR is not impaired after repeated injections and thus does not explain *in vivo* knockdown failure.

Fab'Ri7-PICM uptake is mediated by the TfR in vitro

We next conducted *in vitro* experiments to investigate at which step between internalization and nuclear delivery our nanoparticle-siRNA formulation was blunted. Fab'Ri7-PICM-siGAPDH failed to induce GAPDH knockdown in N2A cells as measured with a sensitive GAPDH assay (results not shown). In a previous study using a very similar formulation of PICM coupled instead to a human anti-TfR mAb, size, cellular uptake, cellular viability and gene silencing were all validated in PC-3 cells(Felber et al. 2011). To validate *in vitro* our novel Fab'Ri7-PICM formulation, endocytosis studies were performed on mouse N2A neuroblastoma cells. N2A cells were incubated with Fab'Ri7- or UT-PICM (negative control) containing siGLO-Red (500 nM) for 5, 15, 30 and 60 min. A rapid accumulation of TfR-targeted nanoparticles was observed within N2A cells and confirmed the ability of Fab'Ri7-PICM to internalize into TfR-expressing cells at 37°C whereas control UT-PICM were barely endocytosed even after a 60-min incubation period (Figure 30). The absence of signal from siGLO-Red encapsulated in Fab'Ri7-PICM after incubation at 4°C confirmed that the uptake was mediated by an energy-dependent mechanism, consistent with receptor-mediated endocytosis (Figure 31). To determine whether the uptake of siGLO-containing Fab'Ri7-PICM was TfR-dependent and saturable, we pretreated the cells with free Ri7 or a control IgG (Figure 32). The incubation with Fab'Ri7-PICM triggered a robust uptake of siGLO whereas the incubation with UT-PICM left only non-specific non-internalized fluorescence outside of cells (Figure 32A,B,F). Pretreatment with 50 or 200 nM of free Ri7 blocked the internalization of siGLO-Red in Fab'Ri7-PICM to negative control (UT-PICM) levels (Figure 32C,D,F). In contrast, pretreatment with control IgG had no effect on siGLO accumulation induced by Fab'Ri7-PICM.

Fab'Ri7-PICM in endosomal compartments

We next investigated internalization mechanisms of Fab'Ri7-PICM complexes by incubating the nanoparticles during 5, 15, 30 min, 1, 4 and 24 h with N2A cells and conducting confocal

microscopy experiments. It is important to note that, after internalization, the fluorescent signal can originate from either free or PICM-bound siGLO Red since endosomal pH may have triggered PICM disassembly. Moreover, the exact proportion of free vs. PICM-bound siGLO could not be determined. Of particular interest, both PICMs and siGLO Red have nuclear-targeting properties. Our results showed that the siGLO signal rapidly colocalized with TfR, a marker of sorting/recycling endosomes (Figure 33AD). Colabeling of siGLO with TfR remained elevated, reaching its maximum after 4 h and diminishing at 24 h. The decline observed at 24 h potentially suggests that siGLO with/without TfR-targeted PICMs have escaped from sorting/recycling endosomes.

Intracellular trafficking can impact the efficacy of pH-sensitive nanoparticles as pH decreases from 6.0–6.5 in early endosomes to 4.5–5.5 in late endosomes and lysosomes, and thus endosomal escape is expected to vary accordingly (Elsabahy et al. 2009; Yessine et al. 2003; Felber et al. 2011). Colocalization analyses with early endosomal marker EEA-1 (Figure 33 BE) showed that siGLO signal could be found in early endosomes. Relatively low colabeling index suggests that siGLO Red was mainly incorporated in other subcellular compartments.

Nanoparticles internalized by a clathrin-mediated pathway are often sorted to lysosomes (Bareford & Swaan 2007; Sakhrani & Padh 2013; Kafshgari et al. 2015), a process suspected to occur with antibodies undergoing TfR-mediated uptake in BCECs (Bien-Ly et al. 2014). Interestingly, endocytosis of the Fab'-targeted nanovehicle led to partial colocalization with lysosomal marker LAMP-1 (Figure 33 CF). Quantification based on images acquired by confocal microscopy showed a colabeling index between siGLO signal and LAMP-1 increasing over time, but remaining low even after 24 h of incubation with N2A cells. This result suggests that PICMs were either recycled back to the plasmic membrane or accumulated into others subcellular compartments. Of note, a clear colocalization of siGLO Red and DAPI nuclear stain was not encountered at any incubation time.

In summary, our results have confirmed that PICMs targeting the TfR are appropriate vehicles to rapidly carry and accumulate nucleic acids into BCECs after a single systemic injection. However,

gene-silencing experiments did not lead to a reduction in protein levels, while endosomal escape and nuclear access of siGLO Red was prevented.

Discussion

Over the past ten years, evidence of the implication BCECs in neurodegenerative disease is growing (Deane et al. 2004b, Persidsky et al. 2006, Weiss et al. 2009a, Devraj et al. 2016). Therefore, directly targeting dysfunction or pathological abnormalities of BCECs could lead to the development of new approaches to successfully treat many brain pathologies (Kuwahara et al. 2011). Indeed, in Alzheimer's disease, many proteins present within BCECs such as RAGE (Du Yan et al. 1996, Deane et al. 2004b) or BACE1 (Devraj et al. 2016) are believed to play a critical role in the establishment of the pathology and directly treating BCECs with siRNA against those targets could result major in therapeutic outcomes.

Previous studies with a PICM formulation almost identical to the one used in the present study, but conjugated to an Fab' anti-human CD71, have not only confirmed the lack of cellular toxicity and ferrying capacity of TfR-targeted PICMs but also their silencing efficiency in PC-3 cells (Elsabahy et al. 2009, Felber et al. 2011). Given the pH-sensitive nature of these PICMs, internalization and accumulation into endosomal compartments would be useful from a BCEC-targeted drug delivery perspective. Endosomes have a lower pH (~5-6.5) than systemic circulation and using a nanoparticle programmed to release its content at endosomal pH could thus enhance the amount of material released within BCECs (Drummond et al. 2000, Yessine et al. 2007, Felber et al. 2011).

In the present work, we report *in vivo* evidence of TfR-targeted PICM delivery of siRNA into murine BCECs. Indeed, systemically administered nucleic acids protected within PICMs were incorporated into BCECs 30 min after a single injection. Moreover, using the fluorescent dsRNA analog siGLO-Red, our results clearly show a rapid, TfR-specific and energy-dependent internalization in N2A cells. However, colocalization studies suggest that Fab'Ri7-PICM may avoid disassembly and thus prevent the endosomal escape of siGLO Red as well as its transit to the nucleus. This could explain why no reduction of GAPDH protein levels was observed in gene silencing experiments.

Since systemic administration of naked nucleic acids generally leads to rapid degradation by nucleases and induces interferon responses (Hornung et al. 2005, Robbins et al. 2009), we conducted *in vivo* experiments to assess the capacity of PICMs to protect and ferry siRNA into the brain. Using a fluorescent dsRNA (siGLO Red), we were able to characterize the brain distribution of

the nanoparticle content. Our microscopic analysis demonstrated the systemic stability of Fab'Ri7-PICMs as BCECs were labeled with siGLO fluorescence after a single i.v. injection of the TfR-targeted dsRNA. These data are in accordance with our previous work showing that Ri7 mAbs accumulate into brain microvasculature (Paris-Robidas et al. 2011, Alata et al. 2014, Paris-Robidas et al. 2016). Scarce evidence of fluorescent signal outside brain vasculature was observed and we cannot rule out a possible colocalization with neurons and astrocytes. However, such low brain penetration is unlikely to be sufficient to trigger a therapeutic effect in non-endothelial cell populations of the brain.

In this study we were not able to observe a significant reduction in the protein levels of GAPDH of mice treated with anti-GAPDH siRNA within Fab'Ri7-PICMs. However, GAPDH mRNA levels were not monitored and thus we cannot rule out a possible impact of our treatment on mRNA levels. Furthermore, given the lack of consensus in the literature on gene silencing protocols, the absence of GAPDH reduction might simply reside in the injected dose (Kumar et al. 2006, Kumar et al. 2007, Xia et al. 2007, Kuwahara et al. 2011). In a study by Kuwahara et al., a repeated injection of siRNA concentration lower than 10 mg/kg were insufficient to induce gene silencing activity (Kuwahara et al. 2011).

Since PICMs owe their gene-silencing ability to their capacity to respond to lower pH by disassembling and releasing negatively-charged siRNA that are free to escape endosomes and reach the nucleus, we performed *in vitro* experiments to validate the cellular uptake of Fab'Ri7-PICMs and their transit in N2A cells. Here, we show that Fab'Ri7-PICMs were internalized by an energy-dependent mechanism, which was inhibited by preincubating cells with free anti-TfR antibody. These observations with N2A cells are consistent with our previous work quantifying cellular accumulation of fluorolabeled Ri7 mAb targeting the TfR (Alata et al. 2014, Paris-Robidas et al. 2016) or luciferase expression with immunoliposomes (Rivest et al. 2007). Moreover, our results provide additional information about internalization mechanisms of TfR-targeted PICM.

Our subsequent microscopic analysis showed that Fab'Ri7-PICMs are endocytosed and mostly integrated into sorting/recycling endosomal compartments in N2A cells. Typically, once nanoparticles are endocytosed, they are predominantly degraded in lysosomes or recycled for extracellular clearance (Medina-Kauwe et al. 2005). It has been proposed that high-affinity anti-TfR mAbs can

impair intracellular trafficking of the TfR by triggering lysosomal degradation of both mAb and its receptor in comparison with low-affinity mAbs (Bien-Ly et al. 2014). However, repeated administration of Fab'Ri7-PICM did not lead to reduction of TfR levels *in vivo*. In this case, it rather appears that the transfer of nanoparticles to early endosomes and lysosomes was limited and that Fab'Ri7-PICMs may have been captive from a recycling endosomal/internalization loop (TfR-positive compartment) where pH does not go below 6 (Sorkin et al. 2002, Maxfield et al. 2004). A similar condition is known to occur when TfR are crosslinked by multivalent transferrin molecules (Marsh et al. 1995). Each Fab' is monovalent but several of them per nanoparticle make PICMs multivalent. Moreover, transferrin itself releases its iron in sorting endosomes but remains bound to its TfR in recycling endosomes and back to the plasma membrane (Marsh et al. 1995). Incorporation in "later" endosomes, which normally takes a few minutes rather than hours (Sorkin et al. 2002, Maxfield et al. 2004) is crucial for PICM disassembly, as downstream endosomal compartments have even lower pH, reaching 5 in late endosomes and 4 in lysosomes (Sorkin et al. 2002). Indeed, acidic pH protonates carboxylate groups of the MAA, causing destabilization of the nanoparticle and promoting endosomal escape of the nucleic acids (Yessine et al. 2003, Hong et al. 2006). On the other hand, massive and rapid accumulation in the lysosome could lead to the degradation of nanoparticle content, thus limiting the release of the therapeutic agent in targeted cells. Live-cell experiments would be necessary to confirm the fate of siGLO molecules, which remains unclear. However, there is no indication that they successfully reached the nucleus, as a clear colocalization with DAPI nuclear stain was never encountered at any incubation time. Overall, our data support the contention that Fab'Ri7-PICM can be effectively used to carry therapeutic genetic material into BCECs. In the present work, our fluorescence microscopy analysis does not have the resolution to ascertain the subcellular compartment reached by free/bound siGLO *in vivo*. However, data obtained from our *in vitro* colocalization analyses suggest that siGLO, and by extension siRNAs, do not transit to the nucleus and are therefore inoperative. The major difference between our Fab'Ri7-PICM formulation and the one that successfully knocked down Bcl-2 in PC-3 cells (Felber et al. 2011) resides in the antibody used for conjugation. The answers to understanding this discrepancy in TfR instrumentalization lie in future studies concentrating on Ri7 trafficking post internalization.

Conclusion

Developing new approaches to enable delivery of biopharmaceuticals to the brain is a major scientific challenge. The present study provides evidence that a novel formulation of TfR-targeted PICMs has the ability to ferry nucleic acids in large amount to the cerebral vasculature. However, more studies are needed to really open the door to the development of new TfR-based strategies for gene therapy to overcome the burden of neurodegenerative diseases based on the treatment of endothelial pathologies.

Acknowledgements

This work was supported by grants from the Canadian Institutes of Health Research (CIHR) (FC—MOP84251, MP—MOP246453), the Alzheimer Society Canada (FC—ASC 0516), and the Canada Foundation for Innovation (10307). The work of FC was supported by a New Investigator Award from the Clinical Research Initiative and the CIHR Institute of Aging (CAN76833).

Figures

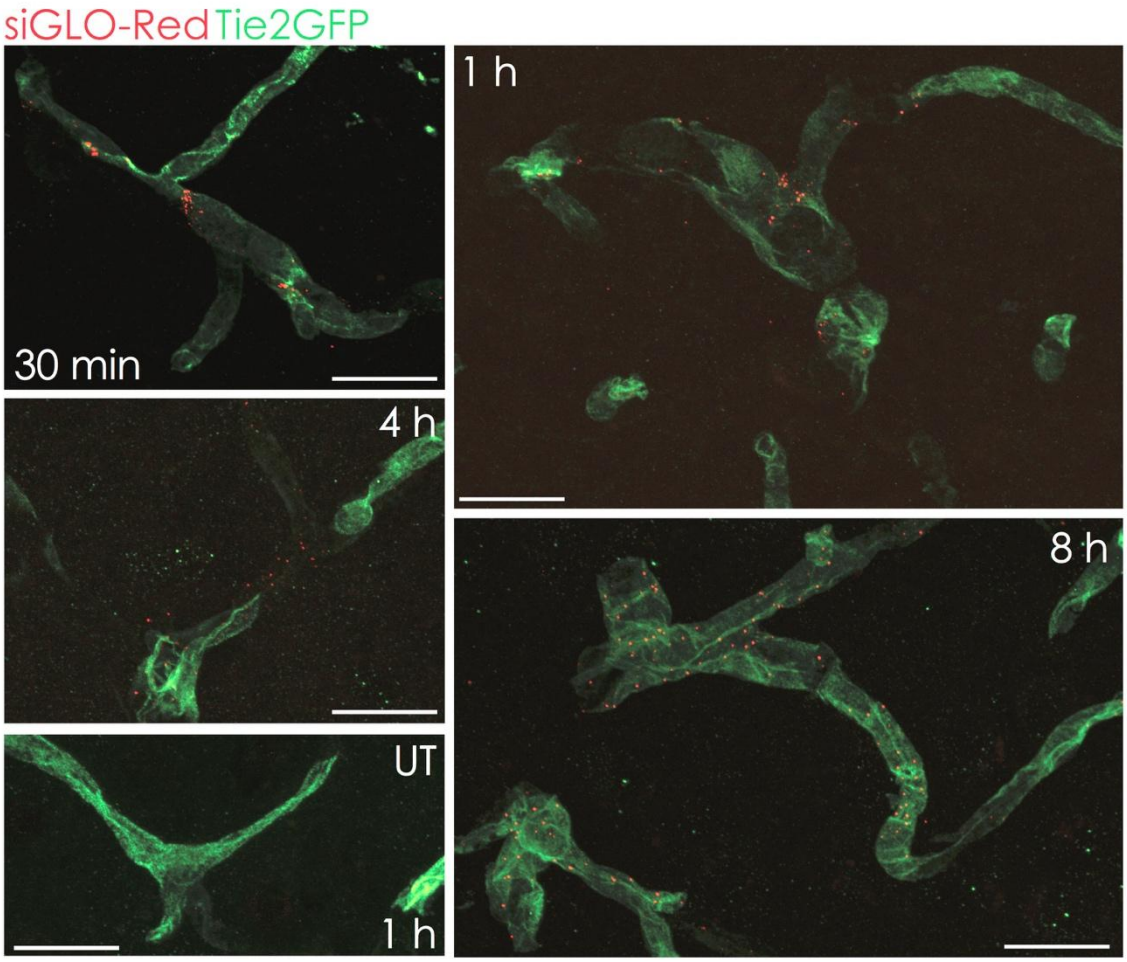

Figure 33: Ri7-targeted PICMs administered systemically accumulate into BCECs.

Tie2GFP mice were intravenously injected with Ri7-targeted PICMs containing siGLO siRNA (red) and sacrificed 0.5, 1, 4 or 8 h post injection. Colocalization analysis shows a strong accumulation of Ri7-PICM containing siGLO (red) within BCECs (green) up to 8 h post-injection. Scarce accumulation of siGLO signal was observable outside brain vasculature (shown by arrows). No apparent fluorescent signal the brain of mice injected with UT-PICM is visible, n = 3. Scale bar = 20 µm.

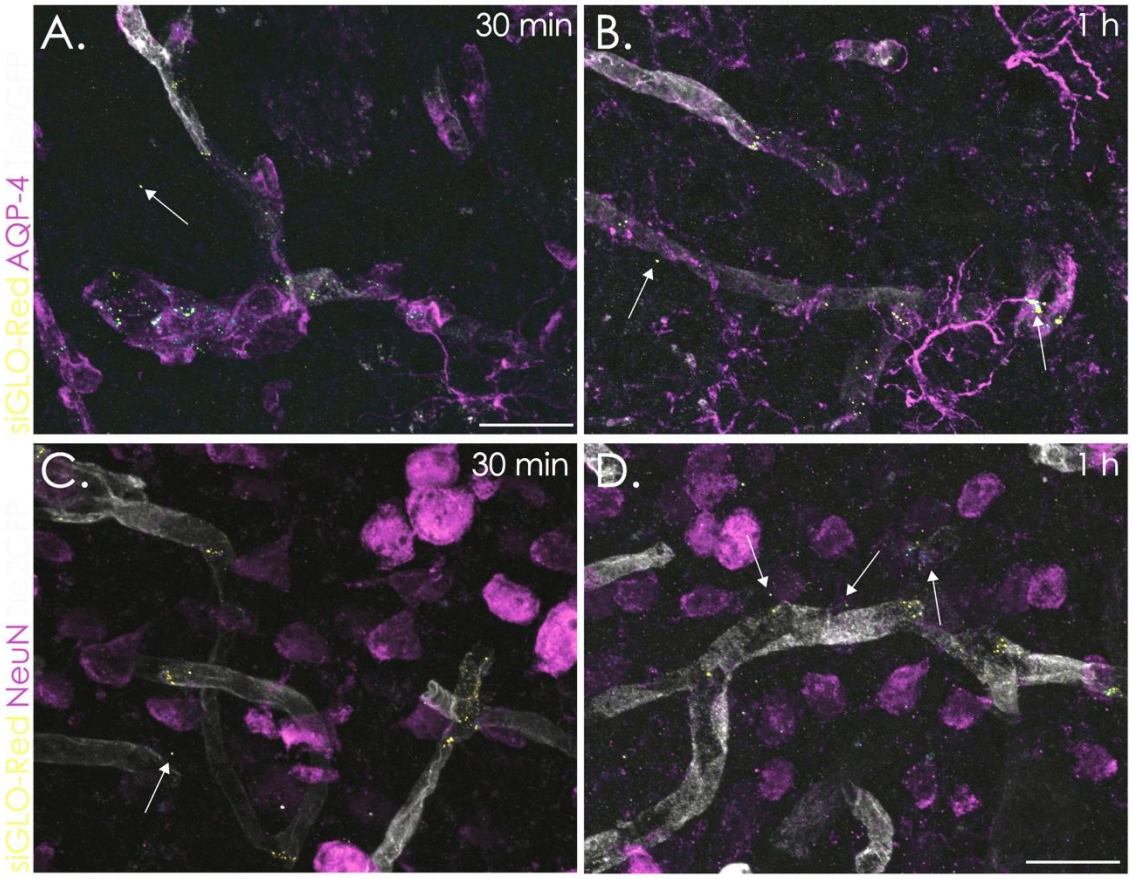

Figure 34: Very limited siGLO siRNA signal outside brain microvessels
Tie2GFP mice were intravenously injected with TfR-targeted PICMs containing siGLO (yellow) and sacrificed 0.5 or 1 h. **(A-D)** Colocalization analysis shows few evidence of accumulation (shown by arrows) **(B)** in astrocyte endfeets (AQP-4, magenta) and **(D)** in neurons (NeuN, magenta) of Fab'Ri7-PICM containing siGLO (yellow). Scale bar = 20 µm.

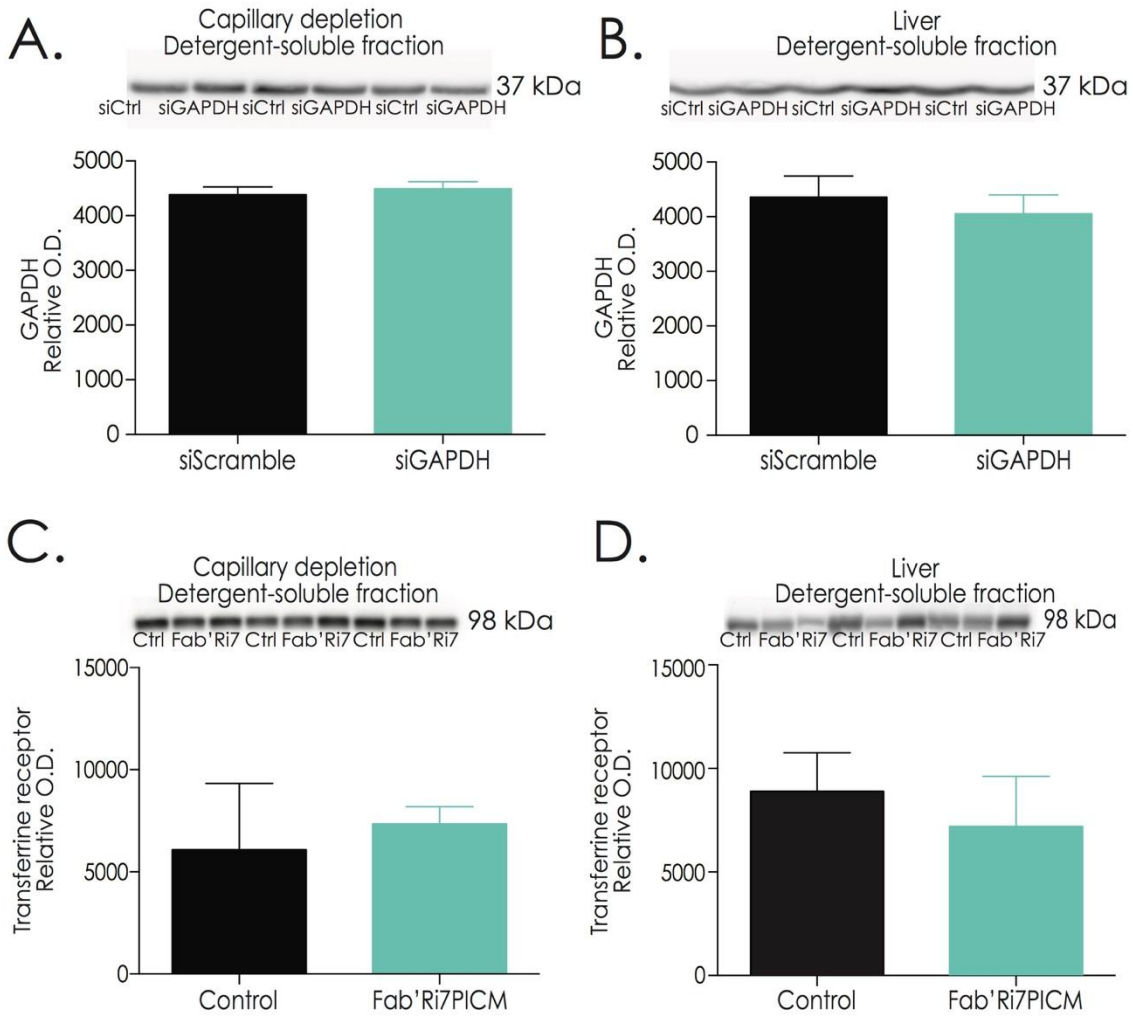

Figure 35: Repeated administration of Fab'Ri7-PICM-siRNA do not lead to reduced GAPDH expression *in vivo*

Mice were injected every 12 h during 36 h with Fab'Ri7-PICM containing 50 µg siRNA targeting GAPDH or a negative control siRNA. **(A-B)** Levels of GAPDH were measured by Western blot on detergent-soluble homogenates from concentrated capillary fractions and in detergent soluble homogenates from the liver, n = 3. **(C-D)** Levels of TfR were measured by Western blot on detergent-soluble homogenates from concentrated capillary fractions and in detergent soluble homogenates from the liver, n = 3 for control and 6 for Fab'PICM injected mice. Statistical comparison: Student t-test. Data represented are means SEM.

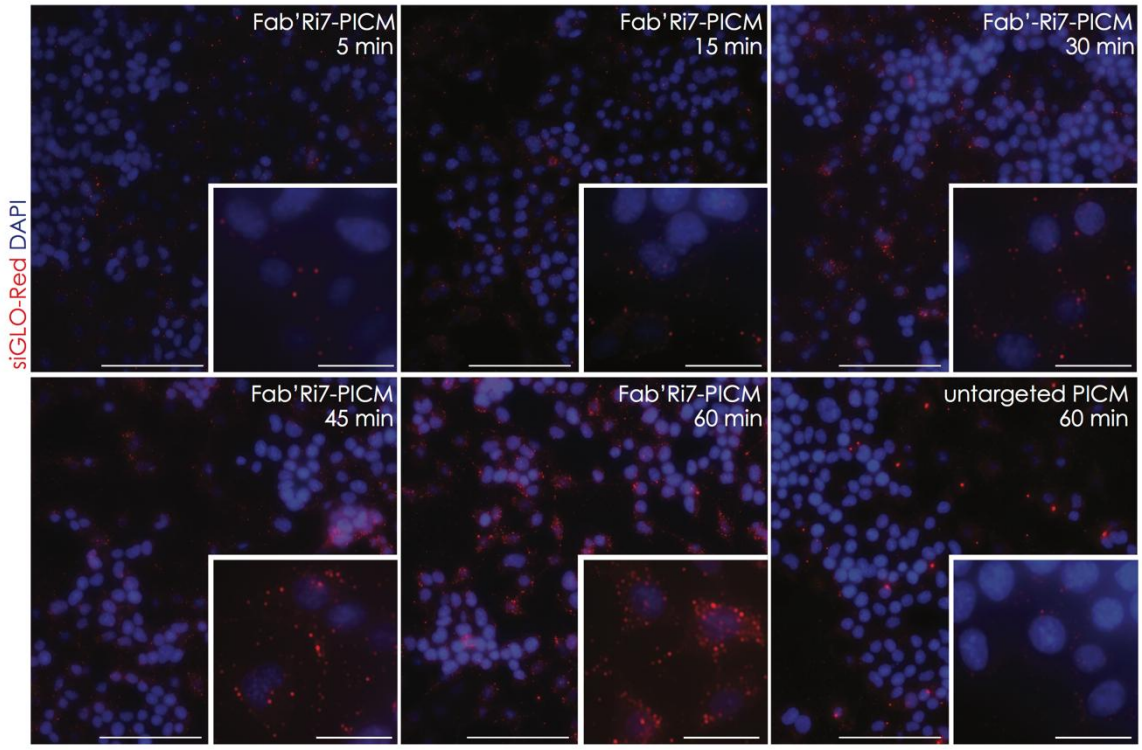

Figure 36: Accumulation of TfR-targeted PICMs in N2A cell lines.
N2A cells were seeded in 96-well plates containing DMEM and 10% FBS. Two days later, they were exposed to Ri7-PICM or untargeted PICM containing siGLO siRNA (red) (500 nM) for (5, 15, 30, 45 and 60 min). Cells were then washed with cold PBS, fixed with 4% PFA and stained with DAPI (blue). n = 2 per condition. Scale bar = 25 µm

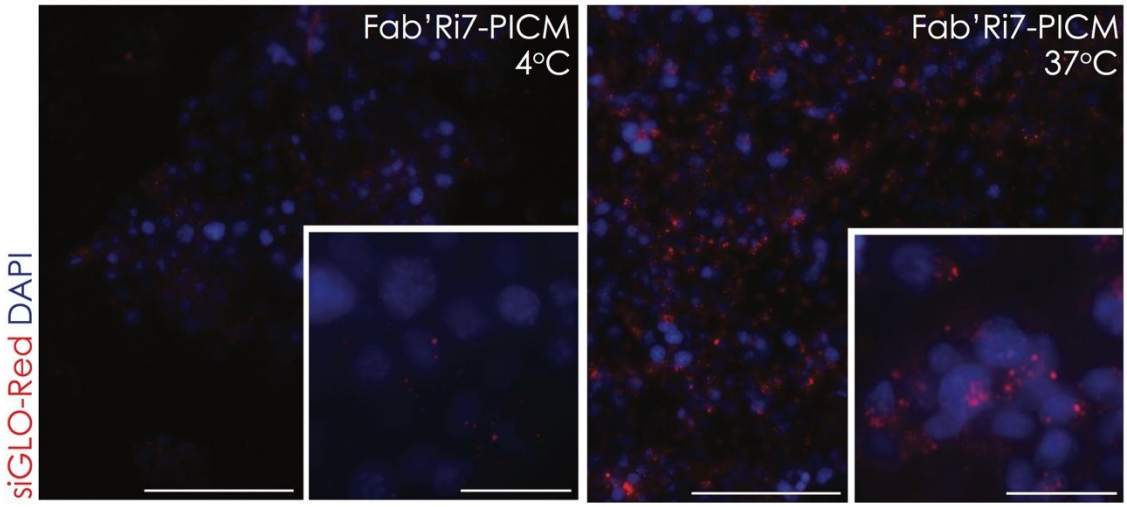

Figure 37: TfR-targeted PICM internalization is mediated by an energy-dependent mechanism. N2A cells were seeded in 96 well plates containing DMEM with 10% FBS. Two days later they were exposed to Ri7-PICM or untargeted PICM containing siGLO (red) (500 nM) for 60 min at either 4°C or 37°C. Cells were then washed with cold PBS, fixed with 4% PFA and stained with DAPI (blue). Scale bar = 100 µm and 25 µm for higher magnification.

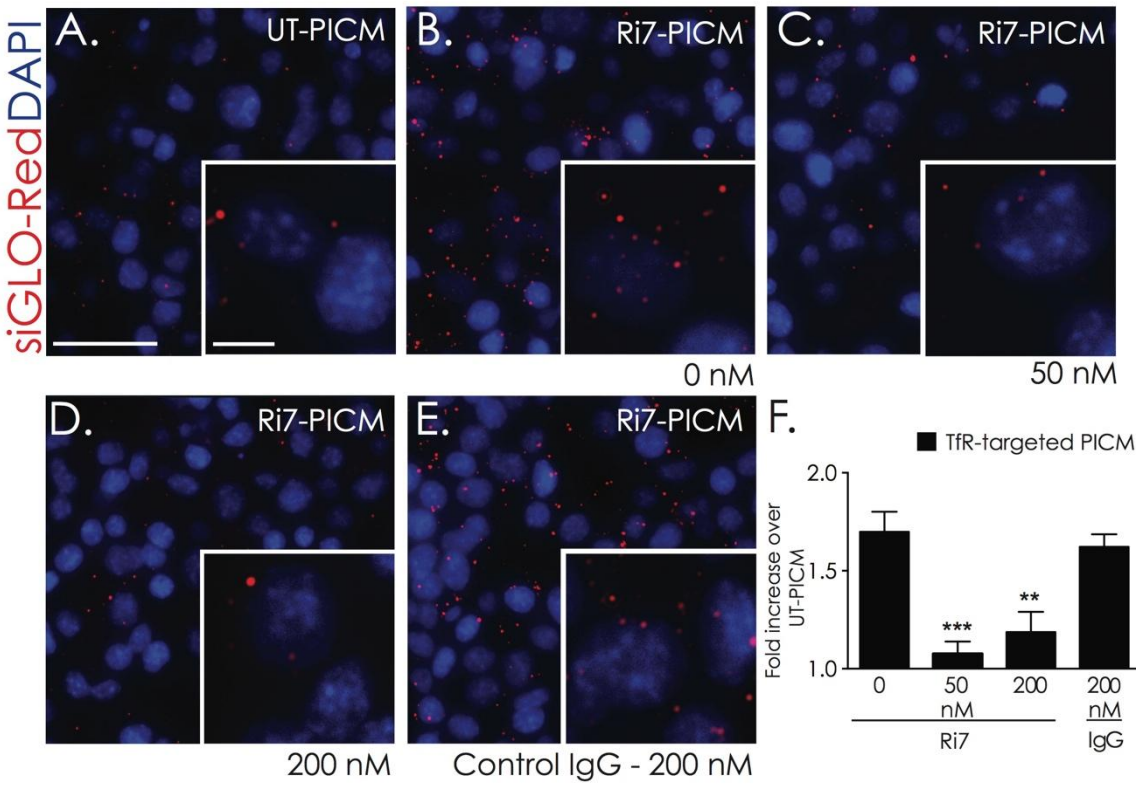

Figure 38: Transferrin receptor-mediated accumulation of Ri7-PICM in N2A cells.
N2A cells were seeded in 96-well plates containing DMEM and 10% FBS. Two day later, they were exposed to Ri7-targeted PICM or untargeted PICM containing siGLO siRNA (red) (500 nM). Representative micrographs following the 15-min incubation with **(A)** untargeted PICM, **(B)** TfR-targeted PICM without or with a 30-min pretreatment with **(C)** 50 or **(D)** 200 nM of free Ri7 and **(E)** 200 nM of control IgG. **(F)** Histogram representing siGLO fluorescent signal quantification showed that the incubation with the untargeted PICM induced a slight accumulation of siGLO whereas the incubation with TfR-targeted PICM led to a robust accumulation of siGLO. Pretreatment with 50 or 200 nM of free Ri7 decreased the accumulation of siGLO following the incubation with TfR-targeted PICM, whereas a pretreatment with 200 nM of control IgG hadno effect. *** $p < 0.001$ (one-way analysis of variance followed by a Tukey's post hoc test). Error bars indicate S.E.M., n = 3 per condition. Scale bars: 50 µm and 10 µm for inserts.

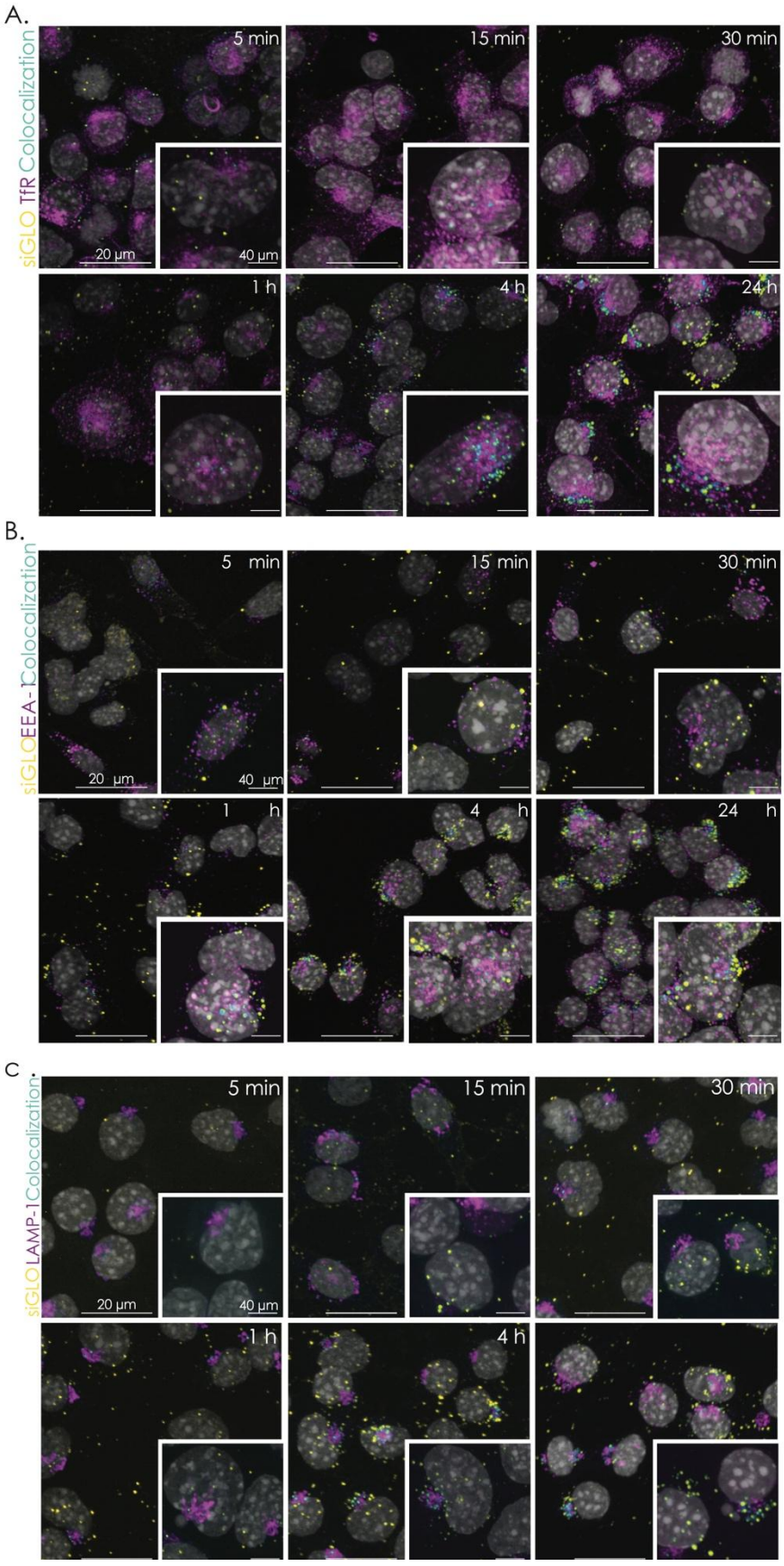
A.
siGLO TfR Colocalization
5 min
15 min
30 min
20 µm
40 µm
1 h
4 h
24 h
B.
siGLO EEA-1 Colocalization
5 min
15 min
30 min
20 µm
40 µm
1 h
4 h
24 h
C
siGLO LAMP-1 Colocalization
5 min
15 min
30 min
20 µm
40 µm
1 h
4 h

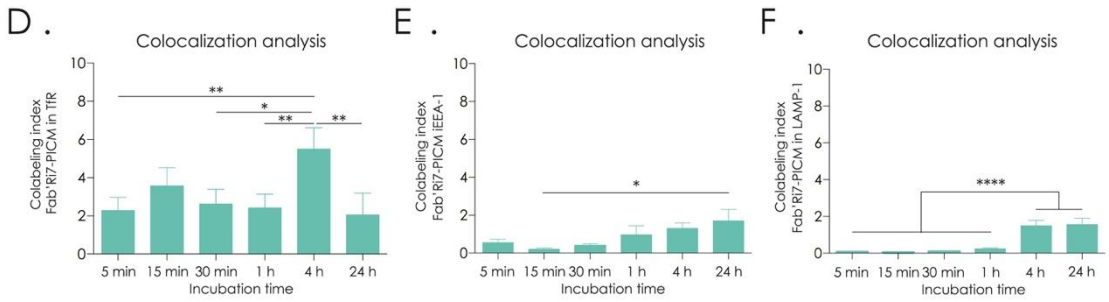

Figure 39: Intracellular trafficking of Ri7-conjugated PICMs.

N2A cells were seeded in µ-Slide VI$^{0.4}$ chamber slides containing DMEM and 10% FBS. Cells were incubated with Ri7-PICM containing siGLO (yellow) (500 nM) for 5, 15, 30 min, 1 h, 4 h and 24 h. **(A-C)** Representative images of the colocalization between Fab'Ri7-PICM (yellow) and TfR, early endosome marker EEA-1 or lysosomal marker LAMP-1 (magenta) through time. Cell nuclei were counterstained with DAPI (white). **(D-F)** Shows colocalization analysis of Fab'Ri7-PICM within TfR, EEA-1 or LAMP-1 labeling. * $p < 0.05$, ** $p < 0.01$ and **** $p < 0.0001$ (one-way analysis of variance followed by a Tukey's post hoc test). Error bars indicate S.E.M, n = 3-6 images per time point. Scale bar = 20 or 40 µm for higher magnification.